Journal of Materials Chemistry C

Accepted Manuscript

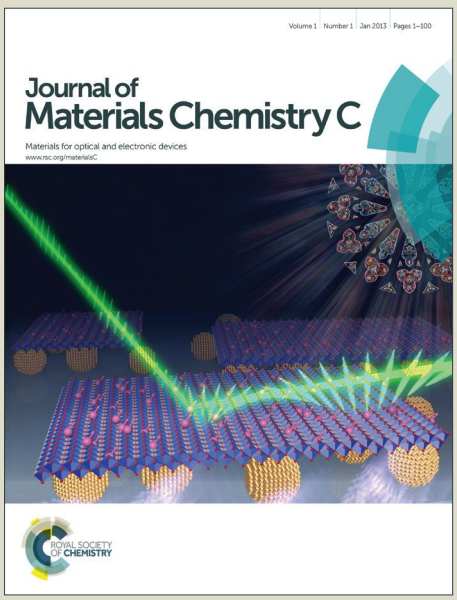

ROYAL SOCIETY OF CHEMISTRY

www.rsc.org/materialsC

Flexible and Transparent Optically Anisotropic Film Based on Oriented Assembly of Nanofibers

Zhijun Ma*[1, 2], Zhongliang Hu[1], Hang Zhang[1, 2], Mingying Peng[1, 2], Xin He[3], Yang Li[1,2], Zhongmin Yang[1, 2], Jianrong Qiu[1, 2]*

[1]State Key Laboratory of Luminescent Materials and Devices, South China University of Technology

[2]Special Glass Fiber and Device Engineering Technology Research and Development Center of Guangdong Province, Guangzhou 510640, China

[3]School of Applied Physics and Materials, Wuyi University, Jiangmen 529020, China

*Correspondence: Zhijun Ma, zhijma@scut.edu.cn; Jianrong Qiu, qjr@scut.edu.cn

Abstract: Nanofibers are characterized with unique electronic, magnetic and optical properties, due to their extremely high aspect ratio and large specific surface area. Assembly of nanofibers with predesigned macro architectures is a key step forward practical applications. Herein, we demonstrate the scalable oriented assembly of nanofibers based on electrospinning, and explore the potential application in constructing optically anisotropic film. By post soaking-and-drying approach, the nonwoven films assembled by oriented polymer nanofibers can be readily converted to flexible films with high transparency, which show optical transmission contrast exceeding 0.9 in the visible to near infrared region. The method for preparation of optically anisotropic films proposed here circumvents the sophisticated dye-doping and thermal drawing processes which are inevitable in conventional approaches. Considering the scalability potential of the electrospinning technique, the method demonstrated here is promising for industrial production of film polarizers.

Keywords: Optical Anisotropy, Nanofiber, Electrospinning, Self Assembly, Film Polarizer

1. Introduction

As one of the most important one-dimensional nanomaterials, nanofibers are characterized with extremely high aspect ratio and two-dimensional confinement, which render them unique electronic, magnetic and optical properties [1-5]. Meanwhile, their continuously long morphology also makes it ideal for energy transport, for example, the conduction of electrons, phonons and photos, etc. In many cases, the molecular or crystalline orientation in nanofibers contributes to inducing anisotropic properties, for example dichroism [6-8]. Although the fabrication of various kinds of nanofibrous materials have been realized with considerable yield and quality, one big obstacle that hampers their future applications is the efficient assembly of nanofibers to construct macroscopic materials and devices with desired functionalities [9]. Rational strategies are urgently needed to construct nanofibers assemblies with expected collective properties, and meanwhile to form nanoscale building blocks at a reasonable scale.

Electrospinning is currently acknowledged as one of the most versatile techniques that suitable for massive production of continuously long fibers of diameters ranging from several nanometers to a few micrometers [10-12]. One unique advantage of this technique is that synchronous fiber assembling can be realized during the fabrication procedure conveniently [13]. Structures packed by electrospun nanofibers assemblies are widely applicable in the fields of environmental remediation, new energy developing, tissue engineering, etc [14-16]. By employing elaborately designed collectors, well aligned nanofibrous assemblies can be easily fabricated by electrospinning, which is especially useful in constructing materials with anisotropic chemical, physical or biological properties. Several groups explored the possible applications of oriented assemblies of electrospun nanofibers. Huang et al. [17] prepared BPDA-PDA PI nanofibrous mats with high mechanical strength via electrospinning, and discovered that both the tensile strength and tensile modulus were improved remarkably when the nanofibers were uniaxially aligned; Yang et al. [18] studied the potential of aligned PLLA electrospun nanofibers in neural tissue

engineering, and discovered that the orientation of nanofibers influenced the elongation of neural cells substantially; Tamura et al. [19] synthesized composite membranes composed of sulfonated polyimide nanofibers and sulfonated polyimide for proton exchange membrane fuel cell, and substantially improved the proton conduction ability of the membrane through alignment of the electrospun nanofibers. Unidirectional molecular or crystalline orientation could be easily realized in electrospun nanofibers [7, 20-22]. By taking advantage of this property of electrospinning, nanofibers with anisotropic optical properties, for example, polarization dependent second-order optical nonlinearity and polarized photoluminescence, have been successfully prepared by several groups [23-26].

Optically anisotropic films, typically the film polarizer, are very important optical devices in a wide range of applications, including planer display, optical navigation and optical communication etc. Taking film polarizer as an example, the representative scattering-types are produced based on a stretched PDLC (polymer-dispersed liquid crystals) film approach [27]. Although the stretched PDLC film technique is simple and suitable for large-scale production, it still faces several limitations. First of all, the polymer for dispersing the LCs (liquid crystals) should be thermoplastic, and meanwhile miscible with the LCs, which poses severe limitation on materials selection. At the same time, the thermal drawing approach requires rigorous control of heating temperature and drawing rate to avoid mechanical breakage of the film, implying high technical challenges. Finally, the finite drawing usually is not able to completely anchor LC molecules to the stretch direction, leading to degradation of the polarization efficiency. Other techniques for making optically anisotropic films, including lithography [28] or coating strategy of thixotropic nanorods gels [29] are not immune to low fabrication efficiency or high cost. Therefore, new efficient approaches are required for fabricating optically anisotropic films with elevated synthetic performance.

Recently, Yao et al. [30] proposed a novel strategy for preparation of efficient optical polarizers by using aligned assembly of PMMA electrsopun nanofibers to induce the orientation of liquid crystals, which was the first report on the electrospun

nanofibers assembly in optical application. Briefly, film of oriented PMMA nanofibers was stacked between two glass slides, then molten LCs were sucked in between the two glass slides to fulfill the inter-fiber voids. Molecular orientation of the LCs was induced by the aligned nanofibers, and stabilized after cooling to room temperature. The final PMMA-LCs-slides composite was rendered with polarizing functionality. This is an instructive work in preparation of optically anisotropic films, which readily circumvented the intricate thermal-drawing process and effectively promoted the polarization efficiency. Nevertheless, glass slides were required in order to hold the nanofibers film and encapsulating the LCs, which deprived the flexibility and increased the thickness of the polarizers, limiting the application scope. On the other hand, the melting-sucking of LCs also makes the fabrication of large-area film polarizers very difficult.

Herein, we propose a new strategy for fabrication of optically anisotropic film also based on aligned assembly of electrospun nanofibers. Different from the strategy proposed by Gu et al., both LCs and glass slides are not needed in our approach. Flexible optically anisotropic film with high transparency and optical transmission contrast are realized simply through soaking the film of aligned electrospun nanofibers in suitable polymer solution and post drying.

2. Experimental

2.1 Electrospinning of Aligned Assembly of Polymer Nanofibers

PVA (Polyvinyl Alcohol, Polymerization Degree=26000, Alcoholysis Degree=97.0~98.0, Viscosity=58-66, n≈1.52) was dissolved in distilled water by rigorous stirring at 60 ℃ in an oil bath pot to form the spinning sol. The mass concentration of the spinning sol was controlled to be 5wt%, 7wt% and 10wt%, in order to study the influence of the concentration on the morphology and orientation of the electrospun fibers. During the electrospinning, the spinning sol sealed in a plastic syringe gauged 20mL was pushed out by a micro-injection pump, and fed into a stainless-steel capillary applied with a positive bias of 12 kV. The feeding rate of the

spinning sol was kept to be 1mL·h^{-1}. An aluminum drum driven by a motor and applied with a negative bias of 8 kV was employed to collect the electrospun fibers. The rotating speed of the collector was adjusted to be 0 rpm, 1000 rpm, 2000 rpm and 3000 rpm, to investigate its influence on the orientation of the electrospun fibers, while the collecting time was varied from 1h to 2h, and finally to 3h to tune the thickness of the nanofibrous films. The nonwoven PVA nanofibrous films were peeled off the drum cautiously and kept for preparation of the optically anisotropic films.

2.2 Preparation of Flexible Optically Anisotropic Films

The as prepared PVA nonwoven films were cut into predesigned sizes, then soaked in PVP (Polyvinyl Pyrrolidone, Mw≈1300000, n=1.51) ethanol solution in a PVDF dish with a concentration of 0.05g·mL^{-1}. The PVP solution containing the PVA films was shifted into an oven and baked at 50 □ until the solution was thoroughly dried. The volume of the PVP solution was controlled to insure the PVA nonwoven films being completely embedded after through drying. The dry and transparent PVA-PVP composite films were carefully peeled off the bottom of the PVDF dish and clipped at the edges to get desired shapes and sizes.

2.3 Characterization

Micro morphologies of the PVA electrospun fibers were observed with SEM (Scanning Electron Microscopy, Nova NanoSEM 430) at the working voltage of 10kV. Optical transparency of the PVA-PVP composite films was evaluated by testing the transmission spectrum with a Perkin Elmer Lambda 900 UV-vis-IR spectrometer. Images of the PVA-PVP film under polarized light source were recorded by a Leica TCS SPE polarizing microscope. To investigate the optical anisotropy of the films, 447nm, 532nm, 633nm and a 808nm continuous-wave LED lasers were adopted as the light source, while a pair of crossed polarizers were applied as the polarizer and analyzer, respectively. A ThorLabs PM320E optical power meter was used to measure

the light power after the analyzer. The PVA-PVP films were placed between the polarizer and the analyzer parallel to their planes. The light power was recorded by the power meter every time after the PVA-PVP film was rotated by 5°. All the experiments for evaluation of the films' polarizing performance were conducted at a constant temperature of 25 □ and a constant humidity of 50%. Polarized Raman spectrum was employed to investigate the molecular orientation in PVA electrospun fibers. Briefly, the PVA nonwoven film was placed on the sample stage with its plane perpendicular to the light path, and the Raman spectrum was recorded every time after the sample was rotated by 5°.

3. Results and Discussion

Figure1(a) schematically illustrates the strategy for the fabrication of optically anisotropic film proposed here. First of all, PVA sol with varied concentrations was electrospun into fibers with mean diameters ranging from 200nm to 750nm. During the spinning, an aluminum drum driven by an electrical motor was employed to collect the fibers, in order to make the fibers oriented. The collected fibrous films are usually not transparent, due to the serious diffraction at the fiber-air interfaces. To make transparent films, the fibrous films were soaked in polymer (such as PVP, PMMA and PVB) solution, dried with the solution in an oven, and finally formed transparent film at the bottom of the PVDF container. Figure1(b) shows the digital photo of the electrospun fibrous film collected with a drum rotating speed of 3000rpm with the size of length×width=300mm×75mm. The film was white and opaque. Figure 1(c) shows the SEM image of the film. The fibers preferentially oriented along the direction as the white arrow instructs. After simple soaking and drying treatment, flexible and transparent film was prepared. Figure 1(d) shows the digital photo of a typical film polarizer composed of PVA fibers and PVP matrix. Limited by the size of the PVDF container, the film polarizer prepared here was sized 75mm×45mm×0.25mm (Length×Width×Thickness). Even larger film can naturally be fabricated when collecting drum and container for soaking with bigger sizes are

employed.

For electrospinning, concentration of the spinning solution is an important factor that influencing the morphology of the nanofibers. The concentration of the PVA solution used in our experiments was set to be 5wt%, 7wt% and 10wt%, respectively. Figure2(a)-(c) show the SEM images of the corresponding samples collected with a rotating speed of 3000rpm. For the sample of 5wt%, the diameter distribution of the fibers was relatively narrow, over 94% fibers were included in the range of 100nm and 300nm (Fig.2(d)). However, the diameter along single fiber was not so uniform, a considerable number of spindle-shaped bulges appeared on some fibers. When the concentration increased to 7wt%, the diameter distribution of the fibers became even narrower, over 96% fibers distributed in the range of 100nm and 300nm (Fig.2(e)). Meanwhile, the diameter along single fiber also became very uniform. Further increase of the PVA concentration led to serious nonuniformity of the fibers' diameters, spanning from 200nm to 1800nm (Fig.2(f)). Besides, a large part of the fibers conglutinated with each other. Average diameter of the three samples were measured to be 200nm, 280nm and 750nm, respectively. Orientation of the electrospun PVA fibers was also influenced remarkably by the concentration of the spinning solution. When the concentration increased monotonically, the percentage of fibers that oriented within the degree of 20° was 68.3%, 81.7% and 81.7%, respectively (Fig.2(g)-(i)). By overall consideration, the 7wt% concentration was the most suitable in this investigation.

The rotating speed of the aluminum drum and the collecting time are another two important factors that affecting the orientation of the electrospun fibers. As revealed by Figure 3(a)-(c), along with the increase of the rotating speed of the aluminum drum, the orientation degree of the nanofibers was improved monotonically. By measuring 60 pieces of fibers for each sample, the number of fibers that oriented within 20° was 58.3%, 61.2% and 83.3% for the samples collected for 2 hours with the rotating speed of 1000rpm, 2000rpm, and 3000rpm, respectively (Fig.3(d)-(f)). High rotating speed is beneficial to enhance the orientation degree of the electrospun nanofibers. Nevertheless, over high rotating speed leads to peeling off of the fibers from the

collector due to the serious centrifugal force. In this work, it was verified that 3000rpm was an appropriate speed. The collection time also influences the orientation of the fibers. Over long collection time has been found to be harmful in maintaining the orientation degree of the electrospun nanofibers. However, we didn't observe analogous phenomenon in our experiment. Adversely, the percentage of nanofibers oriented within 10° for 1h, 3h and 5h collected samples was measured to be 71.7%, 81.7% and 88.3%, respectively, indicative of a monotonically increasing law (Fig.3(g)-(l)). The intrinsic mechanism of this phenomenon has not been clarified.

The diffraction at the interface of two optical mediums is positively proportional to the refractive index difference of the two mediums. Accordingly, to make the film polarizer more transparent, the polymer for burying the nanofibers assembly should have refractive index close to the one of the nanofibers as far as possible. On the other hand, during the soaking stage, the electrospun nanofibers should maintain their nanofibrous morphology integral, implying that the polymer solution for soaking the nanofibers mat should not be able to dissolve the nanofibers. Therefore, careful consideration was taken in selecting the polymer and solvent for the soaking solution. In this work, PVA was used for electrospinning nanofibers. By careful survey, PVP and ethanol were selected for preparing the soaking solution, because PVP has a very close refractive index (n=1.51) to PVA (n=1.52) among the common polymers and is dissolvable in ethanol, while PVA cannot be dissolved by ethanol. After the PVA nanofibrous mats being embedded by the PVP matrix, highly transparent and flexible composite films were prepared. As exhibited by the inset photo in Figure 4(a), the PVA-PVP composite film sized 75mm×45mm×0.25mm (Length×Width×Thickness) was highly transparent, its average transmittance over the range of 400nm to 1400nm was measured to be 91% (shown in Figure 4(a)). The PVA nanofibrous film used for this sample was prepared with the PVA solution concentration of 7wt%, collector rotating speed of 3000rpm and collection time of 3h. Images of the PVA-PVP composite film recorded by polarizing microscope are presented in Fig. 4(b1) and (b2). Bright yellow image of the film with distinguishable fibers orientation can be clearly observed when polarization direction of the light was parallel to the fiber

orientation, while only very dark image with no detail of the fibers was recorded when the light polarization angle was perpendicular to the fiber orientation, indicating the effective polarizing ability of the film. For convenience, small films based on PVA nonwoven mates prepared with different PVA solution concentrations (5wt%, 10wt%) but the same electrospinning parameters (3000rpm-3h) and with the same PVA solution (7wt%) but different electrospinning parameters (1000rpm-2h, 2000rpm-2h, 3000rpm-1h, 3000rpm-2h, 3000rpm-3h and 3000rpm-5h) were also prepared, of which the corresponding digital photos are shown in Figure 4(c1)-(c8). All the samples are highly transparent. A cross-sectional SEM image of the PVA-PVP composite film by cutting the film in the direction perpendicular to the orientation of the PVA nanofibers is shown in Fig. 4(d1). As pointed by the green arrows, the contact between the PVA nanofibers and the PVP matrix was very tight, indicating high affinity between PVA and PVP, which made great contribution to the high transparency of the composite film. In Fig. 4(d1), it also can be observed that the PVA nanofibers buried in the PVP matrix maintained their nanofibrous morphology very well. The PVA nanofibrous mat was extracted from the PVA-PVP film through soaking in ethanol repeatedly and post drying. Its SEM image is presented in Fig. 4(d2). This result clearly demonstrates that both the morphology of the PVA nanofibers and their orientation were maintained quite well after soaking in PVP-ethanol solution and post drying.

Optical anisotropy of the samples was characterized between two crossed polarizers. Intensity of the light (I) transmitted after the analyzer can be expressed by the following equation:

$$I = I_0 \mathrm{Sin}^2 2\theta \mathrm{Sin}^2 \frac{\pi d \Delta n}{\lambda} \quad \text{.....(1)}$$

Wherein, I_0 denotes the light intensity in the status without the sample and when the polarizer and the analyzer were parallel, θ represents the angle between the polarizer and the orientation of the nanofibers, while d is the thickness of the nanofibrous nonwoven film, and Δn is the birefringence of the film. Figure 5 shows the light transmission as a function of θ using light source of different wavelength. Here, the

film thickness d was measured to be 33μm (d denotes the thickness of the PVA nanofibrous mat). All the curves approximately fit the $\sin^2 2\theta$ variation rule, while the maximal value of the light transmission I/I_0 decreased with the light wavelength increasing, being 0.552, 0.390, 0.356 and 0.207 for 447nm, 532nm, 633nm and 808nm, respectively. The light extinction ratios for different wavelength at θ=0 were recorded to be 0.03, 0.016 0.013 and 0.009, indicating superior polarizing performance of the film as optical retarder. Optical transmission contrast η, expressed as $\eta=(I_{max} - I_{min})/(I_{max} + I_{min})$ (wherein I_{max} and I_{min} represent the maximum and minimum values of I when varying the angle θ) was employed to evaluate the polarizing efficiency of the films. The η value of the film was calculated to be 0.9, 0.92, 0.93 and 0.92 for light of 447nm, 532nm, 633nm and 808nm, respectively, almost at the same level. The film birefringence Δn was calculated roughly to be 0.0036 according to equation (1) and the light intensity at θ=45°. Compared with the reported birefringence of PVA film prepared by mechanical drawing technique (in the level of 0.01~0.05) [31-34], the birefringence of the PVA-PVP film prepared here is much lower. The reason, we speculate, should be ascribed to the fact that the PVA nanofibrous film is very porous, therefore the effective volume ratio of PVA nanofibers in the film polarizer was very small. Though the birefringence value is not high compared with the ones of mechanical drawn PVA film, conventional calcite (Δn=0.17) or even quartz (Δn=0.01) wave plates, the easily adjustable thickness and the versatility of the fabrication approach still make the films prepared here competitive to replace the expensive conventional wave plates in a wide range of applications.

The intrinsic mechanism for origin of the birefringence of the PVA-PVP composite films is believed to be ascribed to the orientation of the polymer molecular chains in electrospun nanofibers [20-22]. The polarized Raman spectrum, which has been applied by other groups to investigate the molecular orientation of polymer, was also employed here [20, 21]. As presented in Figure 6(a), the normalized intensity of the Raman resonant peaks at 2913cm^{-1}, originating from the stretching vibration of the C-H bonds, are obviously different when the polarizing direction of the laser

source was adjusted parallel or perpendicular to the orientation of the nanofibers, wherein the former was higher than the later, implying the physical anisotropy at the molecular scale. By gradually changing the angle between the polarizing direction of the laser source and the orientation of the nanofibers in the range of 0~180°, the normalized peak intensity of the C-H bonds exhibited a polarization-dependent variation approximately fitting the cosθ rule, with the maximum and minimum at the angles of 0°/180° and 90°, respectively (Figure 6(b)). The molecular orientation of polymer chains in an electrospinning process is induced by both the shear force of the spinning jet and the static electrical field [20-22], being very useful in constructing materials with anisotropic optical, electric, magnetic and mechanical properties.

Polarizing effect of the film with PVA nanofibers prepared with PVA solutions with different concentrations and the same electrospinning parameters (3000rpm-2h) was investigated. As shown in Fig. 7(a), when the concentration of PVA solution increased from 5wt% to 7wt%, the maximal intensity ratio of transmitted light (447nm) increased substantially from 0.146 to 0.526, but suddenly dropped to 0.125 when the PVA concentration further increased to 10wt% (the thickness of the PVA nanofibrous film was 50μm, 66μm and 69μm for 5wt%, 7wt% and 10wt% samples, respectively). Fig. 7(b) shows the corresponding variation rule of Δn as a function of the PVA concentration. The value of Δn was calculated to be 0.00112, 0.00175 and 0.00075 for the 5wt%, 7wt% and 10wt% samples, respectively. Considering the SEM images and the relevant counting results in Fig.2, it can be speculated that both orientation and morphology (for example the fiber diameter and diameter distribution) influenced the polarizing performance of the PVA-PVP composite film. However, the intrinsic mechanism still has not been clarified yet. According to the origin mechanism of the optical anisotropy, the birefringence of the film can be tuned by the orientation degree of the fibers realized via adjusting the rotation speed of the collector. Figure 7(c) shows the light transmission as a function of θ for samples prepared with different rotation speed, while a 447nm laser was used as the light source. Along with the increase of the rotation speed from 0rpm to 1000rpm and finally to 3000rpm, the maximal intensity ratio of the transmitted light increased

sequentially, due to increase of the fibers' orientation degree. The corresponding value of Δn was calculated to be 0.0005, 0.0016 and 0.0033, respectively (all the fibers were collected for 3 hours). The origin of the slight birefringence of the film prepared with the PVA fibers collected by a resting drum, we assume, should be ascribed to the anisotropic distribution of the electric field at the surface of the drum, which induced certain degree of orientation of the fibers. Figure 7(d) shows the variation rule of Δn as a function of the collector's rotation speed, which exhibits a roughly linear increasing trend. Naturally, we inspect that higher value of Δn can be achieved if higher rotation speed of the collector be employed. Nevertheless, rotation speed higher than 3000rpm is beyond the scope of the collector used in this investigation. According to equation (1), the optical retardation of the film can be tuned via adjusting the film thickness, which was realized conveniently in this investigation through variation of the collecting time. Figure 7(e) shows the variation of light transmission as a function of fiber collecting time. The maximal ratio of the transmitted light at θ=45° grew remarkably when the collecting time prolonged from one hour to three hours, but the growing trend was slowed down when the collecting time further prolonged to five hours. It seems that a saturation value will be arrived at longer collecting time, which we assume should be ascribed to the intensified absorption of the film. The variation of optical retardation of the films as a function of the collecting time is presented in Figure 7(f), which exhibits a similar rule as the light transmission in Figure 7(e) demonstrates.

4. Conclusion

In summary, we propose a simple and scalable strategy for preparation of flexible and transparent optically anisotropic films based on oriented assembly of electrospun polymer nanofibers and post soaking-drying technology. The as-prepared films show efficient optical retardation performance and transparency in the whole visible and near infrared region. More importantly, the strategy employed here circumvents the technical-demanding dye- (or liquid crystal)- doping and thermal drawing techniques, which is inevitable in conventional approaches for making optically anisotropic films.

Meanwhile, our strategy is universally applicable to other kinds of polymers or even inorganic materials, so long as solvents and combination of materials with matched refractive index and solubility for the nanofibers and the film matrix can be properly selected. Considering the scalability and versatility of the strategy employed here, the flexible optically anisotropic films prepared in this investigation are competitive to replace the expensive conventional wave plates in many applications.

Acknowledgement

This work was financially supported by the National Natural Science Foundation of China (Grant Nos. 51302087, 51472091, 11404114, 61307026), and Fundamental Research Funds for the Central Universities (Grant No. 2014ZM0002).

.

References

1. S. Choi, G. Ankonina, D. Youn, S. Oh, J. Hong, A. Rothschild and I. Kim, *ACS Nano*, 3 [9] (2009) 2623-2631
2. J. Huang and R. B. Kaner, A General Chemical Route to Polyaniline Nanofibers, *J. Am. Chem. Soc.*, 2004, 126, 851-855
3. L. Tong, R. R. Gattass, J. B. Ashcom, S. He, J. Lou, M. Shen, I. Maxwell and E. Mazur, *Nature*, 2003, 426[18/25], 816-819
4. V. Fasano, A. Polini, G. Morello, M. Moffa, A. Camposeo and D. Pisignano, *Macromolecules*, 2013, 46, 5935-5942
5. H. Wu, R. Zhang, X. Liu, D. Lin and W. Pan, *Chem. Mater.*, 2007, 19, 3506-3511
6. N. K. Mahanta, A. R. Abramson, M. L. Lake, D. J. Burton, J. C. Chang, H. K. Mayer and J. L. Ravine, *Carbon*, 2010, 48, 4457 -4465
7. E. J. Ra, K. H. An, K. K. Kim, S. Y. Jeong and Y. H. Lee, *Chem. Phys. Lett.*, 2005, 413, 188-193;
8. Y. Ando, T. Sugihara, K. Kimura and A. Tsuda, *Chem. Commun.*, 2011, 47, 11748-11750;
9. J. Liu, H. Liang and S. Yu, *Chem. Rev.*, 2012, 112, 4770-4799
10. D. Li and Y. Xia, *Adv. Mater.*, 2004, 16[14], 1151-1170;
11. S. Ramakrishna, K. Fujihara, W. Teo, T. Yong, Z. Ma and R. Ramaseshan, *Mater. Today*,

2006, 9[3], 40-50;

12. F. E. Ahmed, B. S. Lalia and R. Hashaikeh, *Desalination*, 2015, 356, 15-30
13. W. Teo and S. Ramakrishna, *Nanotechnology*, 2006, 17, R89-R106
14. R. Gopal, S. Kaur, Z. Ma, C. Chan, S. Ramakrishna and T. Matsuura, *J. Membrane Sci.*, 2006, 281, 581-586
15. V. Thavasi, G. Singh and S. Ramakrishna, *Energy Environ. Sci.*, 2008, 1, 205-221
16. T. H. Qazi, R. Rai and A. R. Boccaccini, *Biomaterials*, 2014, 35, 9068-9086
17. C. Huang, S. Chen, D. H. Reneker, C. Lai and H. Hou, *Adv. Mater.*, 2006, 18, 668-671
18. F. Yang, R. Murugan, S. Wang and S. Ramakrishna, *Biomaterials*, 2005, 26,2603-2610
19. T. Tamura and H. Kawakami, *Nano Lett.*, 2010, 10, 1324-1328
20. M. V. Kakade, S. Givens, K. Gardner, K. H. Lee, D. B. Chase and J. F. Rabolt, *J. Am. Chem. Soc.*, 2007, 129, 2777-2782
21. L. M. Bellan and H. G. Craighead, *Polymer*, 2008, 49, 3125-3129
22. S. Pagliara, M. S. Vitiello, A. Camposeo, A. Polini, R. Cingolani, G. Scamarcio and D. Pisignano, *J. Phys. Chem. C*, 2011, 115, 20399-20405
23. D. V. Isakov, E. M. Gomes, L. G. Vieira, T. Dekola, M. S. Belsley, and B. G. Almeida, *ACS Nano*, 2011, 5, 73-78
24. S. Pagliara, A. Camposeo, E. Mele, L. Persano, R. Cingolani and D. Pisignanol, *Nanotechnology*, 2010, 21, 215304
25. S. Pagliara, A. Camposeo, A. Polini，R. Cingolani and D. Pisignano, *Lab Chip*, 2009, 9, 2851-2856.
26. L. Persano, A. Camposeo and D. Pisignano, *Prog. Polym. Sci.*, 2015, 43, 48-95
27. I. Amimori, N. V. Priezjev, R. A. Pelcovits and G. P. Crawford, *J. Appl. Phys.*, 2003, 93, 3248-3252
28. J. J. Wang, L. Chen, X. Liu, P. Sciortino, F. Liu, F. Walters and X. Deng, *Appl. Phys. Lett.*, 2006, 89, 141105
29. J. Kim, J. Peretti, K. Lahlil, J. Boilot and T. Gacoin, *Adv. Mater.*, 2013, 25[24], 3295-3300
30. Y. Yao, Z. Gu, J. Zhang, C. Pan, Y. Zhang and H. Wei, *Adv. Mater.*, 2007, 19, 3707-3711
31. E. J. Shin, Y. H. Lee, S. C. Choi, *J. Appl. Polym. Sci.*, 2005, 95, 1209-1214
32. W. S. Lyoo, S. S. Han, W. S. Yoon, B. C. Ji, J. Lee, Y. W. Cho, J. H. Choi, W. S. Ha, J. *Appl.*

Polym. Sci., 2000, 77, 123-134

33. T. Tanigami, H. Suzuki, K. Yamaura, S. Matsuzawa, *J. Mater. Sci.*, 1998, 33, 2331-2338

34. C. Sawatari and Y. Yamamoto, *Polymer*, 34, 1993, 956-966

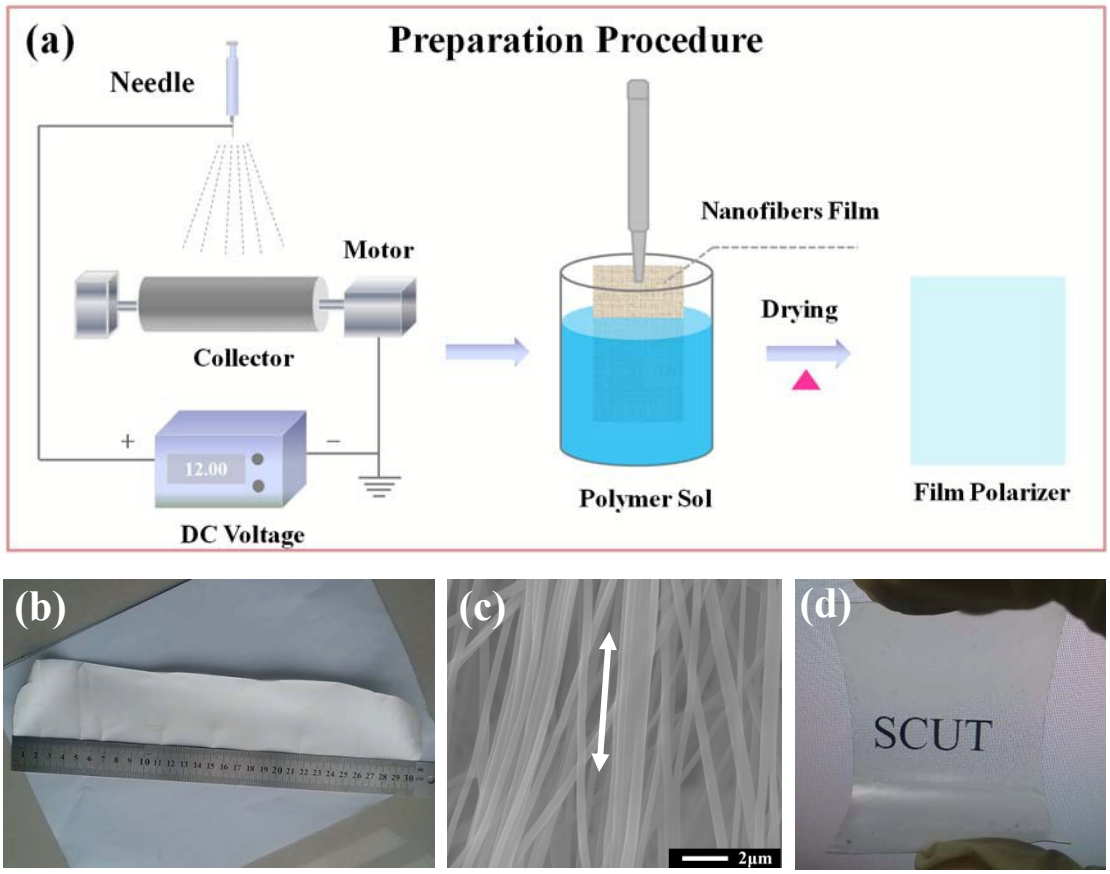

Fig. 1. (a) Schematic illustration of the preparation of the optically anisotropic film based on aligned polymer fibers; (b) Digital photo of the electrospun PVA fibrous film; (c) SEM image of the aligned PVA electrospun fibers; (d) Digital photo of the optically anisotropic film based on aligned PVA electrospun fibers.

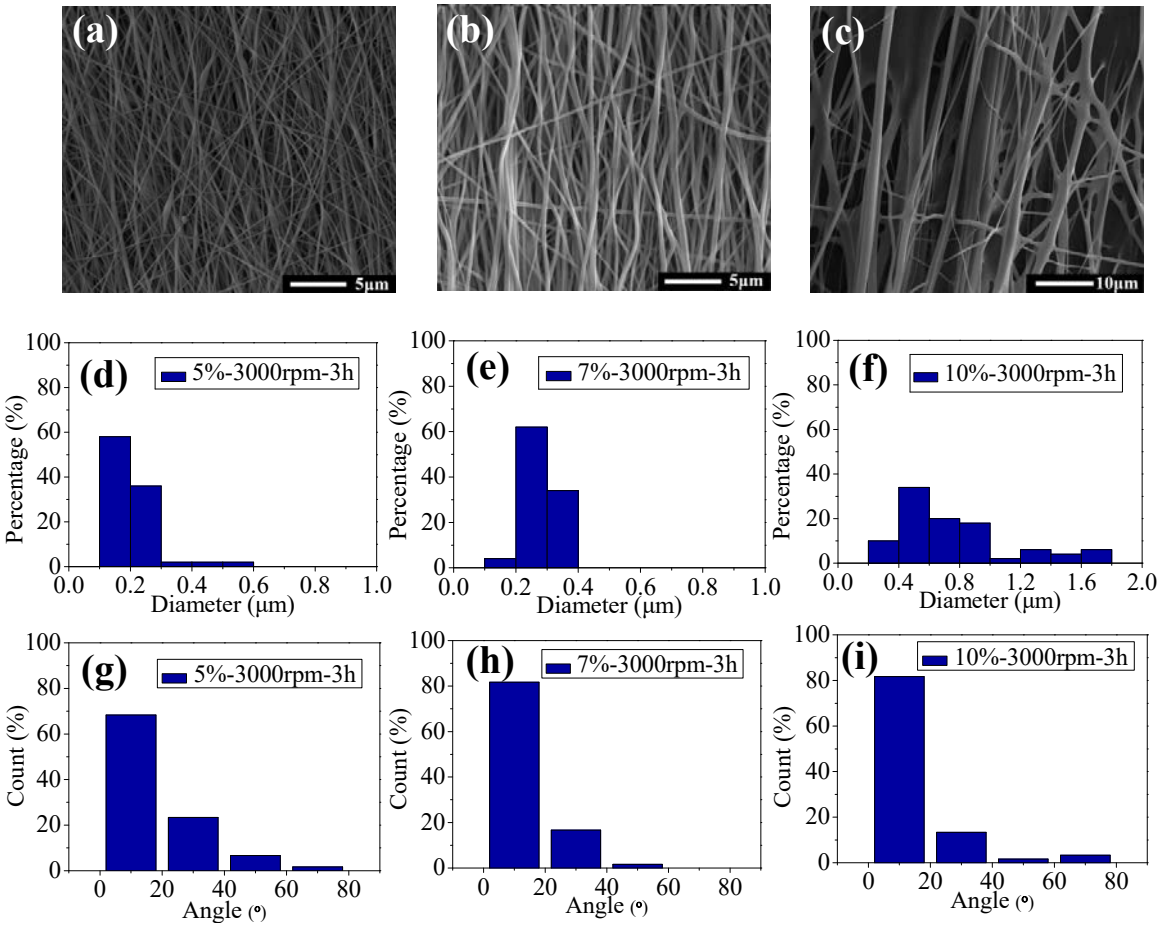

Fig. 2. (a)-(c) SEM images of PVA fibers electrospun with different concentration of the PVA solution ((a): 5wt%; (b): 7wt%; (c): 10wt%); (d)-(f) Diameter distribution of the PVA fibers corresponding to the SEM images of (a)-(c); (g)-(i) Distribution of the orientation angle of the PVA fibers corresponding to the SEM images of (a)-(c).

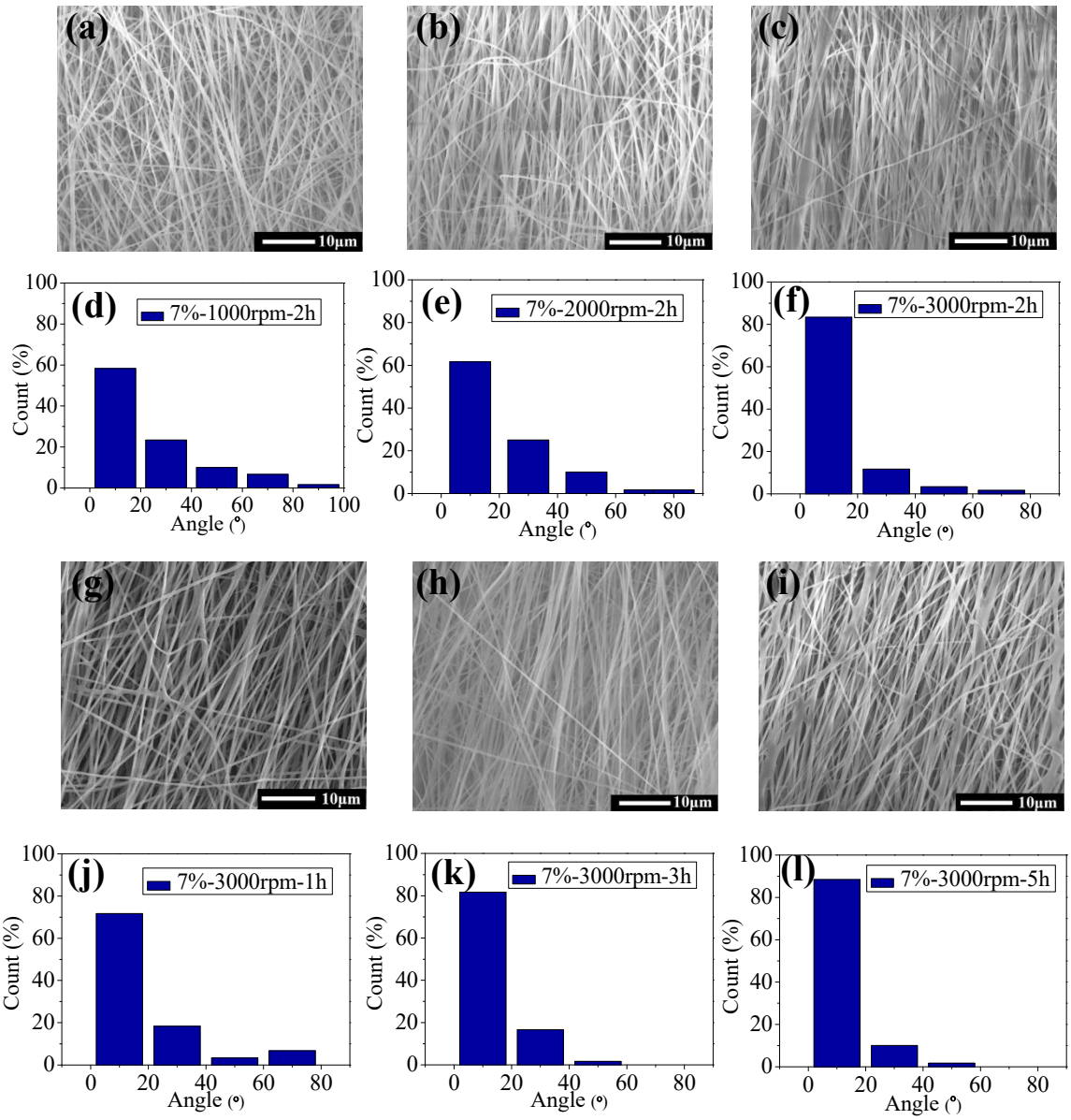

Figure 3. (a)-(c) SEM images of PVA fibers prepared with different rotation speed of the collector and the same collection time of 2 hours ((a): 1000rpm; (b): 2000rpm; (c): 3000rpm); (d)-(f) Distribution of the orientation angle of the PVA fibers corresponding to the SEM images in (a)-(c); (g)-(i): SEM images of PVA fibers prepared with different collection time and the same rotation speed of the collector ((g): 1 hours; (h): 3 hours; (i): 5 hours); (j)-(l) Distribution of the orientation angle of the PVA fibers corresponding to the SEM images in (g)-(i).

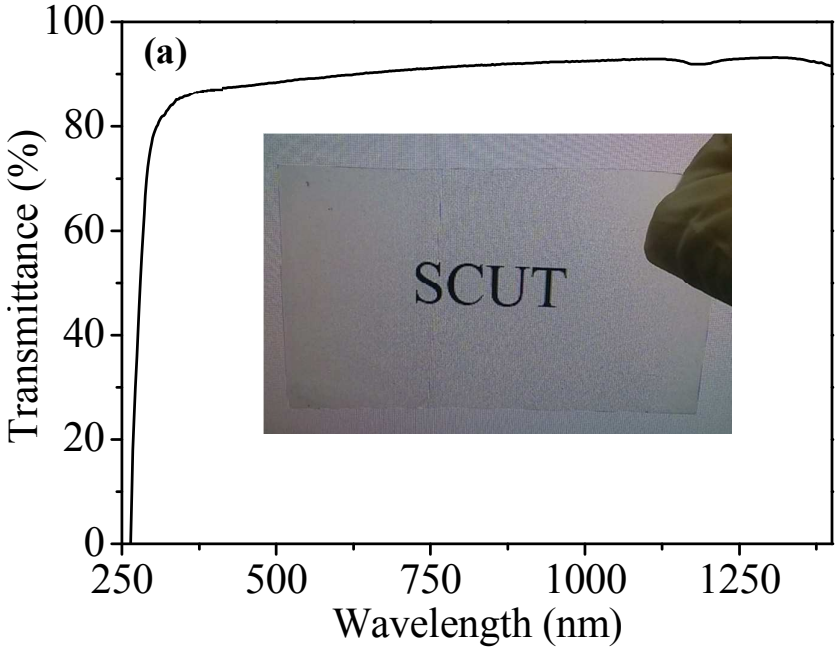

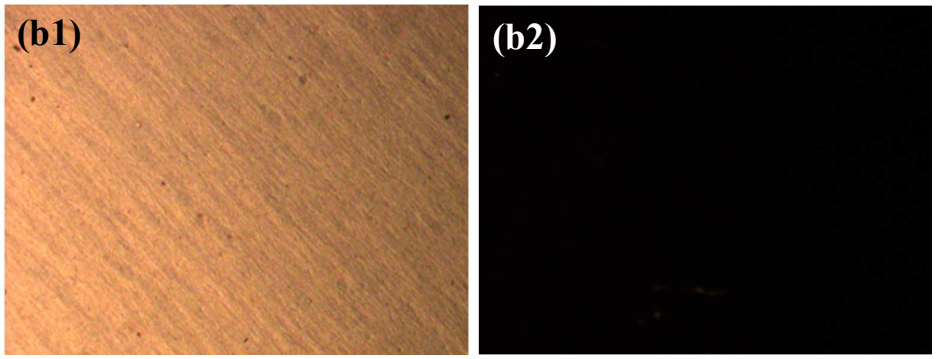

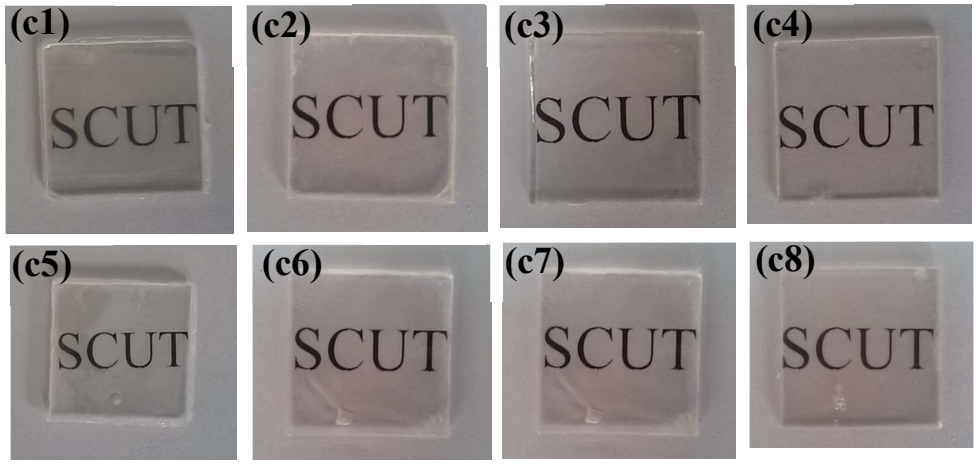

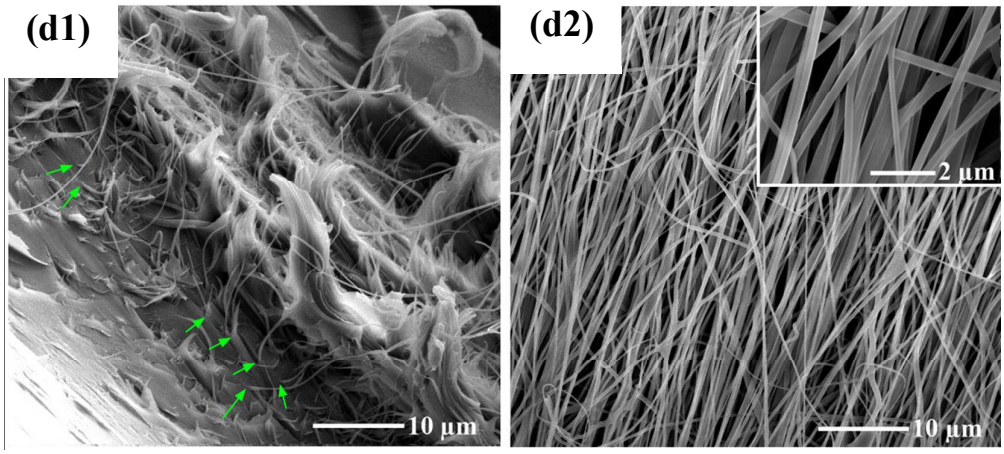

Figure 4. (a) Transmission spectrum of the PVA-PVP optically anisotropic film (The PVA fibers used were prepared with the rotation speed of the collector to be 3000rpm and collection time to be 3 hours, the concentration of the PVA solution for electrospinning was 7wt%); the inset in (a) shows the digital photo of the PVA-PVP optically anisotropic film; (b) polarizing-microscope images of the PVA-PVP composite film (b1: with the light source parallel to the fibers orientation; b2: with the light source perpendicular to the fibers orientation); (c) Digital photos of small-size PVA-PVP optically anisotropic films with PVA fibers prepared with different electrospinning parameters (1-2 were prepared with the PVA fibers in Figure 2(a), (c), 3-8 were prepared with the PVA fibers in Figure 3(a), (b), (c), (g), (h), (i)); (d1) A cross-sectional SEM image of the PVA-PVP optically anisotropic film; (d2) SEM image of the PVA nanofibrous film extracted from the PVA-PVP optically anisotropic film by soaking the film in ethanol and post drying.

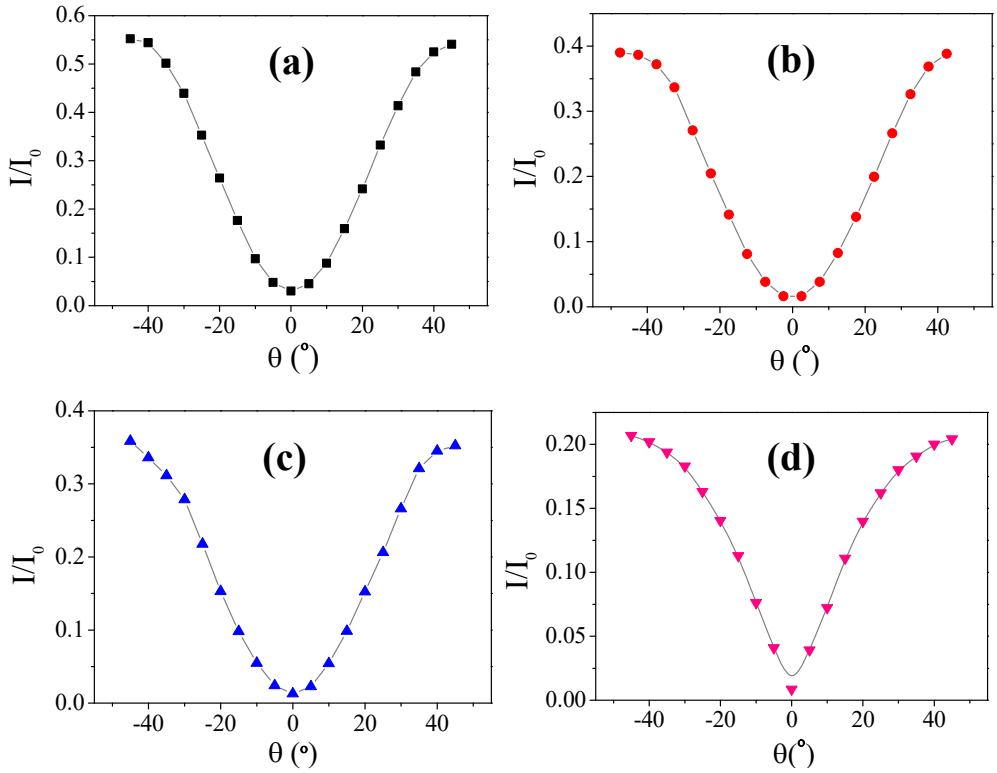

Figure 5. Light transmission of the PVA-PVP optically anisotropic film as a function of θ using light source of different wavelength ((a): 447nm; (b): 532nm; (c): 633nm; (d): 808nm. θ denotes the angle between the polarizer and the orientation of the fibers) (the PVA fibers for this sample was prepared with the rotation speed of the collector of 3000 rpm and collection time of 3 hours, the concentration of the PVA spinning solution was 7wt%).

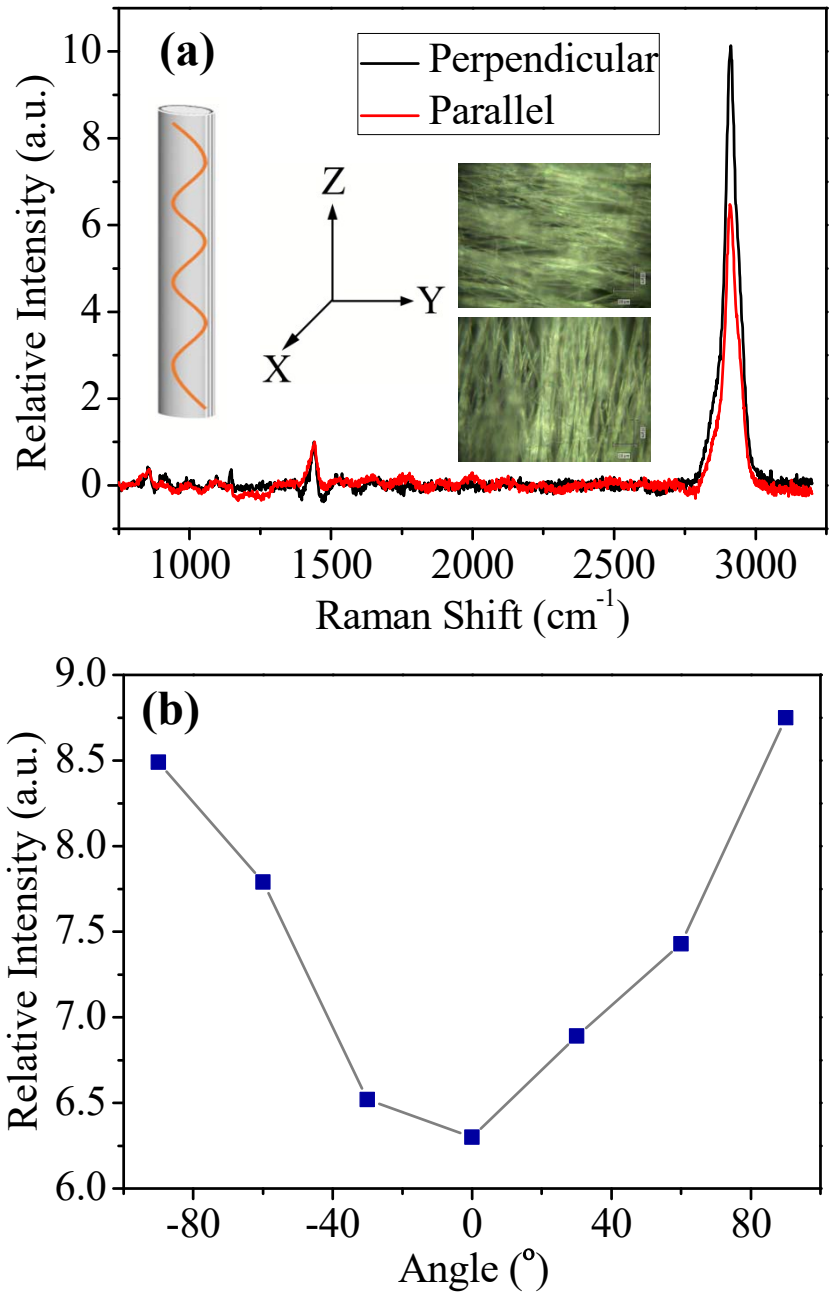

Figure 6. (a) Polarizing Raman spectra of the PVA fibrous mat with the light polarized perpendicular (the black curve) and parallel (the red curve) to the orientation of the fibers, the intensity of the peaks were normalized by the peak centering at around 1440 cm^{-1}; the dark green photos in (a) shows orientation of the PVA fibers, and the figure at the left side schematically shows the molecular structure oriented in PVA fiber; (b) Variation of the relative intensity of the peak of the Raman spectra centering at 2910 cm^{-1} in (a) as a function of the angle between the polarization direction of the light and the orientation of the fibers.

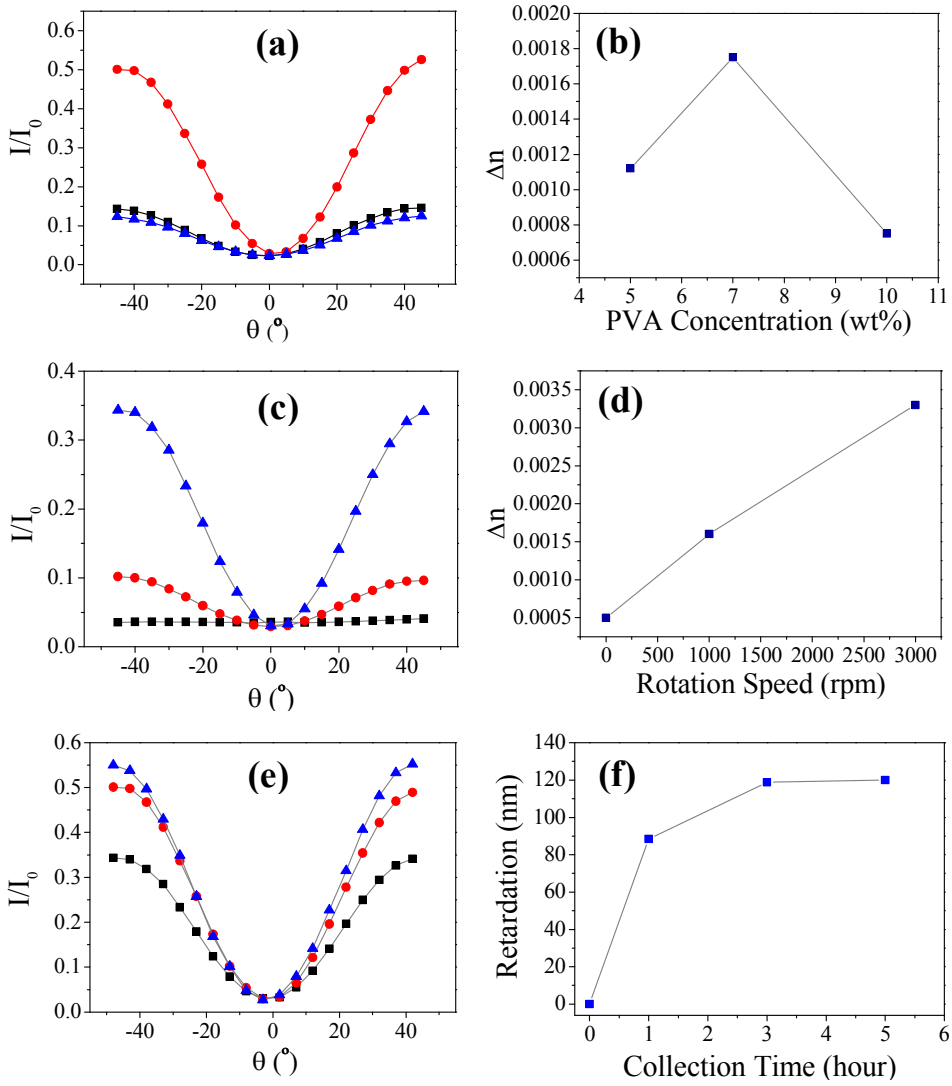

Figure 7. (a) Variation of the light transmission as a function of θ for the samples of PVA fibers prepared with different PVA concentrations and the same rotation speed of the collector (3000rpm) and collection time of 2 hours (black curve: 5wt%; red curve: 7wt%; blue curve: 10wt%. θ denotes the angle between the polarizer and the orientation of the fibers); (b) Variation of birefringence (Δn) of the PVA-PVP optically anisotropic film as function of PVA concentrations; (c) Variation of the light transmission as a function of θ for the samples of PVA fibers prepared with the same PVA concentration, the same collection time of 2 hours and different rotation speed of the collector (black curve: 0 rpm; red curve: 1000 rpm; blue curve: 3000 rpm); (d) Variation of birefringence (Δn of the PVA-PVP optically anisotropic film as function of rotation speed of the collector; (e) Variation of the light transmission as a function

of θ for the samples of PVA fibers prepared with the same PVA concentrations, the same rotation speed of the collector of 3000 rpm and different collection time (black curve: 1 hours; red curve: 3 hours; blue curve: 5 hours); (f) Variation of optical retardation of the PVA-PVP optically anisotropic film as a function of collection time.

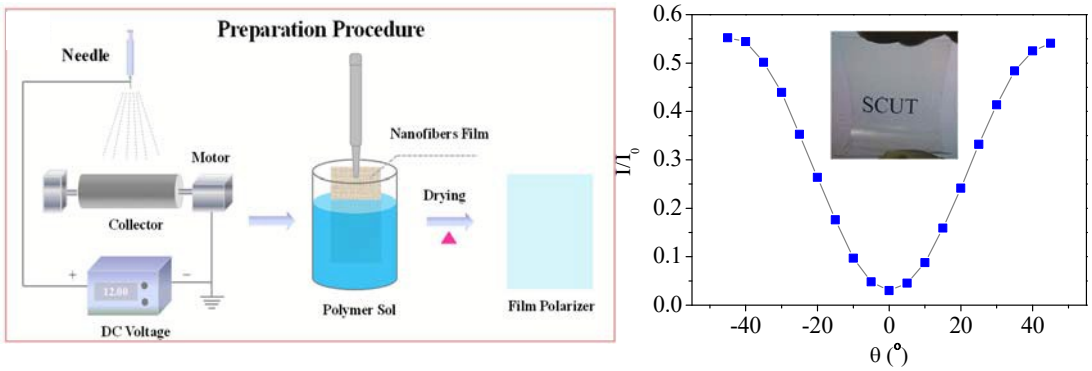

Flexible and optically anisotropic film with high transparency and optical transmission contrast in the visible and near infrared region was prepared based on aligned assembly of electrospun PVA nanofibers and simple post soaking and drying. The strategy for preparation of optically anisotropic film proposed here is simple and scalable, and has the potential to replace the conventional approaches in many applications.